# AUTOSTEREOSCOPIC MEASUREMENT: PRINCIPLES AND IMPLEMENTATION

**Jie Shan, Chiung-Shiuan Fu, Bin Li, James Bethel, Jeffrey Kretsch*, Edward Mikhail**

Geomatics Engineering
School of Civil Engineering
Purdue University
550 Stadium Mall Drive
West Lafayette, IN 47907-2051

## ABSTRACT

Stereoscopic perception is a fundamental requirement for photogrammetric 3D measurement and accurate geographic data collection. Traditional stereoscopic techniques require operators wearing glasses or using eyepieces during the measurement and interpretation process. However, the recent emerging autostereoscopic technique makes it possible to eliminate this requirement. This paper studies the principles and implementation of autostereoscopic photogrammetric measurement. After reviewing the available technologies of autostereoscopic display, we address the principles and properties of backlight autostereoscopic display used in this study. Their possible effects on 3D viewing and measurement are discussed. To accomplish and evaluate autostereoscopic measurement, a 3D toolbox Auto3D is developed that has common photogrammetric functions, such as Y-parallax removal, adjusting x-parallax, point labeling and image rotation. The autostereoscopic measurement is achieved by adjusting the two images until the 3D cursor rests on the exact feature locations of left and right images. To evaluate the performance of the autostereoscopic measurement, images at resolution of 25 and 50 microns are measured by a group of seven students, who are asked to digitize well defined roof and ground points. Results of theoretical study and analysis on the measurements are presented. As a conclusion, the experience on this novel technology is addressed based on the measurement outcome.

## INTRODUCTION

Photogrammetric mapping and interpretation practices have been using stereoscopic techniques for a long time. Although the development of photogrammetry in the past century witnessed three different phases: analogue, analytical and digital photogrammetry, all of them use eyepieces or glasses to obtain stereoscopic view based on which mapping and interpretation are conducted. Recent development in autostereoscopic devices/monitors [Meritt and Fisher, 1993; Petrie, 2001] makes it possible to perform photogrammetric practices without using goggles, eyepieces or other viewing aids.

Early thought on this technology to be used for photogrammetry is presented by [Petrie, 2001]. However, the primary application fields of this technology are collective visualization and image interpretation. The principle for 3D autostereoscopic measurement is not well established. As a result of this, autostereoscopic 3D measurement capabilities are not available; their performance and properties are unknown to the photogrammetric society. This paper will study the principles, properties, implementation and behavior of the autostereoscopic measurement technology as a possible technical alternative in photogrammetric practice.

## AUTOSTEREOSCOPIC PRINCIPLE

3D display technology can be characterized as two types, with glasses and without glasses. The latter is often referred as autostereoscope. In general, the principle of autostereoscopic display may vary from holographic, volumetric, to binocular disparity (Figure 1).

3D images produced by holographic and volumetric approaches match with the apparent spatial position of the corresponding image points. Holography [Fowles, 1989] is a two-step process for the recording and reconstruction of 3D objects. Hologram is a special diffraction screen. It is used to reconstruct the detail of the wave field emitted

* with the National Geospatial-Intelligence Agency

by the object to be imaged. The viewer looking at the hologram sees the image of the object in depth, which can be changed just by moving viewer's head. Volumetric displays project virtual image points to a physical volume of space where they appear either on a real surface, or in translucent images forming a stack of distinct depth planes. In this approach, viewers' eyes fuse these images together to create a seamless 3D view that allows the viewers to walk 360 degrees around the display and see a three-dimensional image.

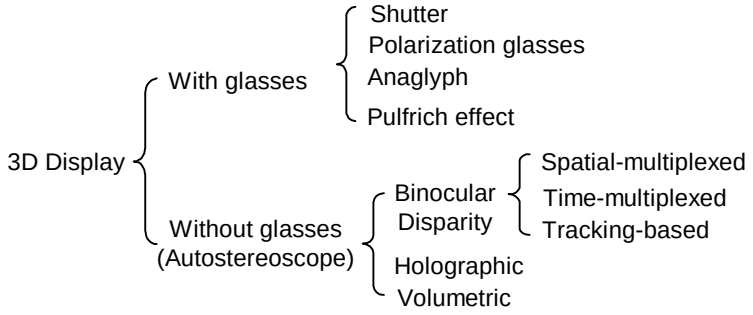


**Figure 1.** Classification of 3D Display based on display principles

Binocular technology can be divided to three categories: time-multiplexed, head tracking and spatial-multiplexed. All of them apply the binocular disparity to fuse the images by brain to produce the sensation of depth from slightly different views of two eyes [Lipton, 1992]. Time-multiplexed is using the capability of human visual system to merge the constituents of a stereo pair across a time-lag of up to 50 ms. The left and right-eye views are shown in rapid alternation and synchronized with an LC-shutter. Tracking-based display can move vertical slits that placed in the focal plane of the lens sheet, and the left and right-eye views are time-sequentially displayed on a CRT screen. The slit position can be switched by moving the display and rotating it around its vertical axis according to viewer's head position. Spatial-multiplexed displays direct the light emitted by pixels of different perspective views to the appropriate eye based on different optical effects like diffraction, refraction and reflection. This type of display can be classified according to technologies such as parallax-illumination displays, lenticular plate, integral imaging, field-lens displays and barrier-grid displays etc.

The most popular technologies in the market are application of parallax-illumination displays and lenticular plate. Parallax barrier shown in Figure 2 can be used to represent the general principle. This principle also reflects the geometry of other similar autostereoscopic implementations, such as lenticular technology. [Okoshi, 1976; 1980].

The autostereoscopic technique is based on the principle of parallax barrier and its derivatives described in [Okoshi, 1976]. As is shown in Figure 2, specially designed images (also called parallax stereogram) are placed behind a barrier made of opaque material with fine transparent vertical slits. The parallax stereogram is composed of interleaving stripes from the left and right images of a stereopair. Each transparent slit will act as a window to the corresponding image stripes. The image and the barrier will be arranged in such a way that the left eye and right eye of the viewer will only see the left image and right image, respectively, so that the stereoscopic effect can be obtained.

Based on this general principle, the lenticular technique uses an array of cylindrical lenticular lenses as the parallax barrier and places it in front of the panoramagram as shown in Figure 3 [Hattori, 1991]. A generalization of these principles may allow for stripes from multiple images to be used to compose the panoramagram or the parallax stereogram for multiple views. Both lenticular and parallax barrier techniques

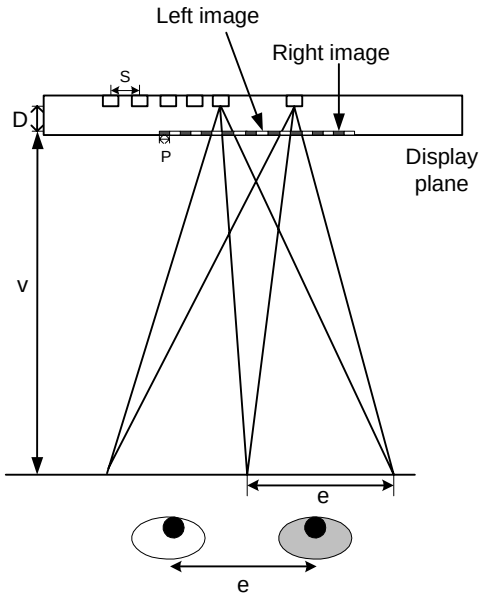


**Figure 2.** Principle of parallax barrier autostereoscope

support multiple views in one scene and provide spatial-multiplexed view while the viewer moves his or her eyes from side to side [Meritt and Fisher, 1993]. (see Figure 4).

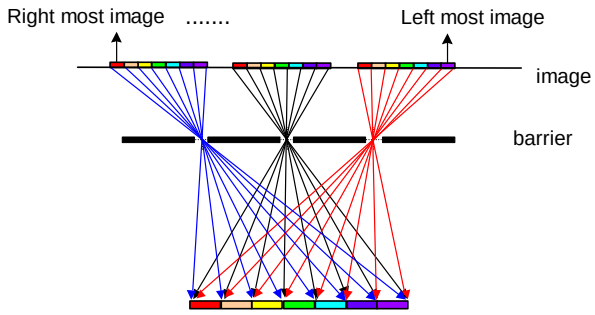


**Figure 4.** Parallax stereogram or panoramagram for autosterescope

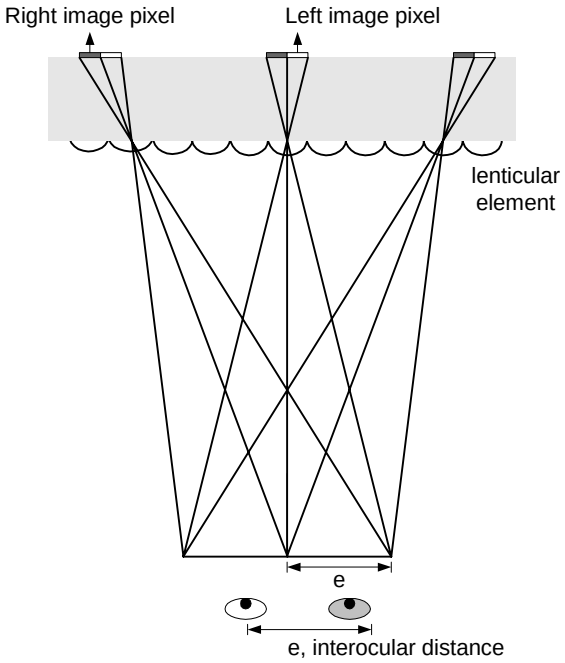


**Figure 3.** Principle of lenticular autostereoscope

The autostereoscopic monitor used in this study is model 2018XL manufactured by DTI, Inc., USA. It uses backlight technique to generate a sequence of light at certain frequency. This is equivalent to the curvature of the lenticular lens being vanishing. In this situation, the lenticular lens becomes flat stripes with a constant interval as illustrated in Figure 2. Unlike other popular autostereoscopic monitors, this monitor supports only two (2) channels, therefore, it has higher resolution than other multi channel displays. Moreover, this monitor is 2D and 3D compatible. When 3D mode is turned off, it can be used as a common 2D monitor. A summary of the main specifications of the DIT monitor used in this study is listed in Table 1. Figure 5 displays the DTI monitor and its control panel used in this study.

**Table 1.** Main specifications of DTI autostereo monitor

| | |
|---|---|
| Display Size | 18.1" |
| Display Type | TFT LCD |
| Max.Display Resolution | 1280x1024 |
| Computer Resolutions Supported | 640x480 @ 60 Hz*; 800x600 @ 60 Hz*; 1024x768 @ 60 Hz*; 1284x1024 @ 60 Hz; 720x400 @ 70 Hz* (PC text mode)<br>* Resolutions other than 1280x1024 are scaled to full-screen. |
| User Controls | 2D/3D; 3D Mode; Stereo Reverse on/off |
| Display Area | 14.1" (W) x 11.3" (H)<br>359.0 mm (W) x 287.2 mm (H) |
| Pixel Pitch | 0.2805 mm (H) x 0.2805 mm (V) |
| Display Colors | 16.7 million (24-bit color, 8 bits/color) |
| Viewing Distance | 29" +/-4"; 71.1 cm +/-10.2 cm |

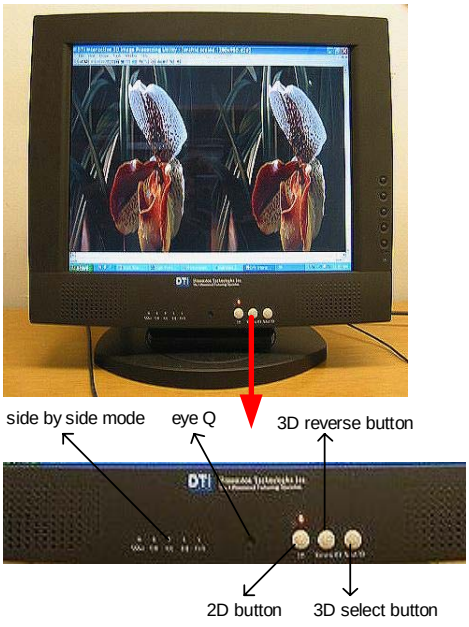


**Figure 5.** DTI 2018XL model and the front panel

## VIEWING GEOMETRY

Despite the fact that various autostereoscopic monitors are available in the market, their viewing properties for photogrammetric observation and measurement are unclear to the photogrammetric society. In the following

sections, these will be investigated through a theoretic reduction and empirical tests by using the DTI monitor. The geometry of autostereoscopic principle is illustrated in Figure 2. For a given monitor design, the following relationship is valid.

$$\frac{e}{v} = \frac{s}{2D} \tag{1}$$

Equation (1) reveals a basic relationship in autostereoscopic viewing [Eichenlaub,1991]. It shows the ratio of eye base and viewing distance needs to be equal to a constant related to the monitor to obtain the best stereo effect. This constant essentially is the ratio of pitch and plate distance to the monitor. This means a viewer of a larger eye base needs to adjust to stay farther away from the monitor. More likely a woman viewer needs to sit herself closer to the monitor than a man does. Similarly, a taller viewer more likely sits farther to the monitor than a shorter one does. In manufacture, the monitors are designed such that the clear focus can be obtained for a common viewer (eye base 65mm) at arm distance (75cm) [Eichenlaub, 1992].

The existence of viewing zone is another property of autostereoscopic observation. Within the viewing zone, a viewer can obtain clear and right stereo effect. Human heads can move horizontally in parallel to the monitor plan. Every movement at an interval of eye base will ensure the right stereo effect. This property implies that multiple viewers can obtain the stereo at the same time, if they are positioned at the right places [Son et al, 2003]. For a monitor with width w and average eye base e, the number of viewing zones *N* can be determined as

$$N = \frac{w}{e} \tag{2}$$

A viewer can adjust his or her position within a viewing zone to receive the best stereo effect. Therefore, it is important to understand the viewing zone properties. Using the coordinate system shown in Figure 6, these can be analytically characterized. The eye base line separates the trapezoid of a viewing zone into two triangles: the front triangle that is for viewer moving close to the monitor, and the rear triangle that is for viewer to move away from the monitor from nominal viewing line.

Figure 6 shows the geometry of viewing zone for a planar autostereoscopic display. For simplicity, we consider the geometry along the center plane of the display only. The coordinate system is positioned the origin in the center of display, the x and y (not shown in the figure) axes are parallel to the display plane, the axis z is as the depth to the viewer and perpendicular to the display plane. The viewer's eyes, left ( L ) and right ( R ), are separated by the distance, e, and are at a viewing distance, v, from the display plane. The best lateral viewing freedom is located at the nominal viewing line. The best vertical (perpendicular to the display plane) viewing freedom is possible as long as the observer's eyes stay within the viewing zone. Usually the best viewing area is as wide as the display plane, and viewing zone R and L located alternately from the center (0,v). While illustrated in 2D, these viewing zones appear as diamond shapes from above. The diamond shape viewing zone can be separated into two triangles, we define them as front triangle and rear triangle as shown in figure 7. For viewing zone n, starting from the center of the monitor and taking $\pm 1, \pm 2, \pm 3, \cdots$ for the left and right part of the screen, their xz coordinates are (see Appendix for details)

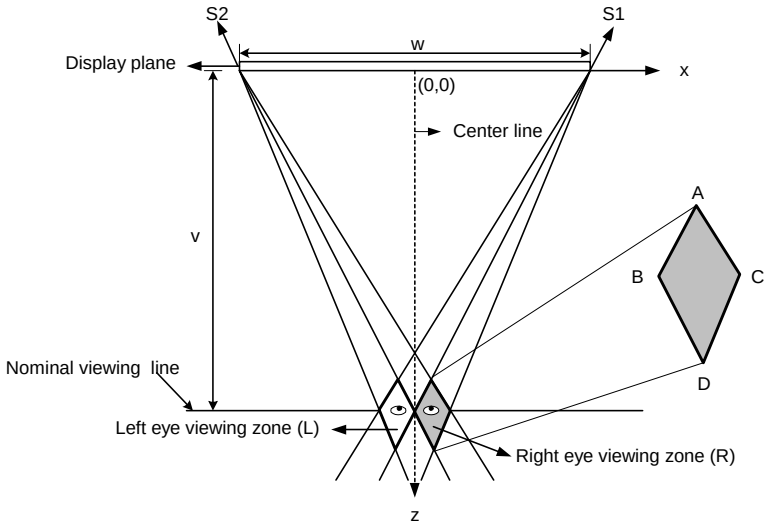


**Figure 6**. Optical geometry model of viewing zones

For the front triangle

$$\left(\frac{(2n-1)we}{2(w+e)}, \frac{wv}{w+e}\right) \tag{3}$$

For the rear triangle

$$(\frac{(2n-1)we}{2(w-e)}, \frac{wv}{w-e}) \tag{4}$$

As shown in Figure 7, the region that head can move with stereoscopic effect is slightly different with the areas defined by the front and rear triangles. The front and rear movements in the depth from the nominal viewing line are expressed by $h_f$ and $h_r$ in Figure 7. These values are determined as

$$h_f = \frac{ev}{w+2e} \tag{5}$$

$$h_r = \frac{ev}{w} \tag{6}$$

The heights of triangles essentially represent the range that a viewer can move perpendicular to the screen to receive the stereo effect. According to equation (5) and (6), this range is dependent on the monitor size, the viewing distance and eye base. It is also shown that the front range $h_f$ is slightly smaller than the rear range $h_r$. In our DTI monitor, the front range and rear range are respectively estimated as 9 and 12.5 cm from nominal viewing line, yielding totally 22cm continuous range for a viewer to adjust his or her position in the direction perpendicular to the screen plane. This study also shows that the trapezoids of all viewing zones have the same area.

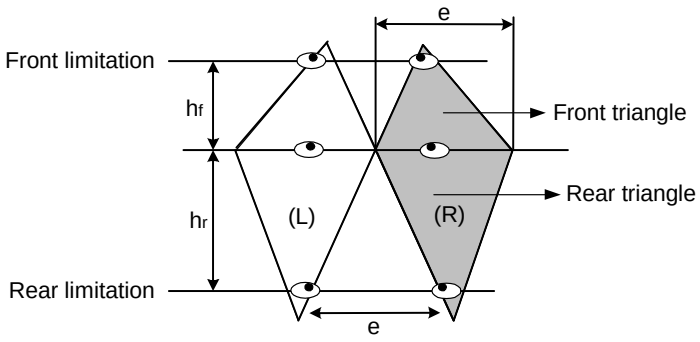


**Figure 7**. Head moving limitation in depth

For the DTI monitor in our study, the number of viewing zone is 7. A viewer can obtain stereo effect in seven locations by adjusting his or her position laterally. It should be noted that these are the locations that perfect stereo effect is ensured. In fact, a viewer can move his or her head outside the range defined by the monitor width. Therefore, there are practically more than 7 zones where viewers can receive stereo effect. However, since the viewing direction is not right perpendicular to the monitor in this situation, the magnitude of the light transmitted to the viewer's eyes is significantly reduced. As a result of this, the stereo view will become darker while the viewer positions are away from the screen center.

## MEASUREMENT PRINCIPLES AND Auto3D TOOLKIT

This section will discuss the geometry to be used for photogrammetry under autostereoscope. It essentially establishes the conversion between screen coordinate system and image coordinate system. After that, classical photogrammetric theory can be used for mapping practice.

The principle of (barrier based) autostereoscopic system requires that the two images of a stereo pair displayed interleaved in columns. In other words, the horizontal resolution of the stereoscopic view is only half of the vertical resolution. As a result of this effect, the two images need to be resampled properly to obtain correct and sharp stereoscope. Two options can be taken in this regard. As the first option, one may take odd columns from the left image and even columns from right image to form the parallax image. This down-sampling process cannot use the full resolution of the original images and may not be allowed for high quality applications. The other option is to duplicate the rows of the two original images. This essentially double the image size for 3D display, however, as a trade-off the resolution of the original images is retained. Under this option, the full resolution of the original images is used.

The objective of image measurement is to obtain the file or image coordinates of interested features. Because the displayed images are interleaved on the monitor, it is inconvenient to record and deduct screen coordinate of the interleaved 3D image directly. Instead, our measurements are recorded as in the original left and right images. As is shown in Figure 8, each image is held by a moving display window which shows the current visible portion of the entire image. Each window has its own cursor and coordinate system. The two image windows are placed side by

side horizontally in the monitor. The interleave process will place and display the odd columns in the left window and even columns in the right window on the monitor when it is switched to 3D mode. It should be noted this process not only displays the images in 3D mode, but all the other contents in the windows such as cursors, symbols and other drawings.

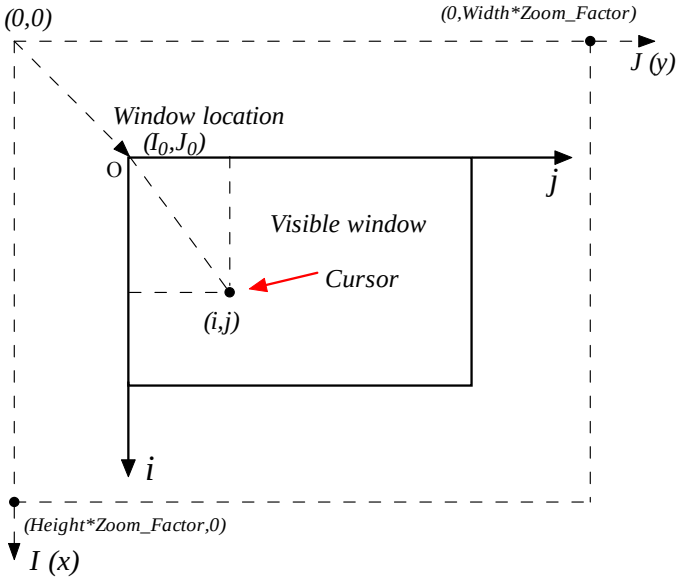


**Figure 8.** File *(I,J)* and window *(i,j)* coordinate systems

$$x = I / zoom\_factor = (I_0 + i) / zoom\_factor$$
$$y = J / zoom\_factor = (J_0 + j) / zoom\_factor \quad (7)$$

Auto3D is a toolkit developed to collect image features under autostereoscopic mode with DTI monitor 2018XL. Its interface is based on Visual C++ 6.0. With Microsoft Fundamental Classes' Multiple Document Interface with Document/View framework, the toolkit can load, display and manipulate two images, conduct autostereoscopic measurement, label and export the results. Figure 9 presents the main image measurement windows. Notice there are four small 2D windows shown at the upper right corner of the left and right image windows. This is designed for mono view as provided by some commercial digital photogrammetric workstations. Users may need them under 3D mode to assure their 3D measurement. The four windows are a duplicate of two 2D image clips from the left and right images, respectively. The two identical left image clips and two identical right image clips are placed respectively at the exact distance of half of the screen width. In this way, they can be viewed without x-parallax under 3D mode.

The floating 3D cursor is specifically designed for the toolkit. The idea is to change the default cursor created by Visual C++ to two cursors at a constant distance by erasing the original one and redrawing them as a cross type cursor. The two cursors are placed at the distance of half of the monitor width to make sure two cursors will overlap under 3D mode. Under 2D circumstance, two cursors will stay in the left and right windows, respectively. The size of cursors is decreased to half width of ordinary one in 2D mode. Once the monitor is switched to 3D mode, the two cursors will be interleaved along with the images and be displayed as a 3D virtual floating cursor. When conducting the stereo measurement, one horizontally moves the images in the left and right 2D image windows by rolling mouse wheel to adjust the x-parallax. This movement allows the viewer to achieve the best depth perception for 3D measurement.

To digitize points and get pixel information for further data analysis, the 3D cursor should be rested just on top of the feature. The viewer can evaluate that by checking the small mono windows. Then viewer can label the feature and record the pixel coordinates from left and right images. The set of coordinates can provide the detailed information about the disparity of the point observer measured, which can be further used for 3D position determination.

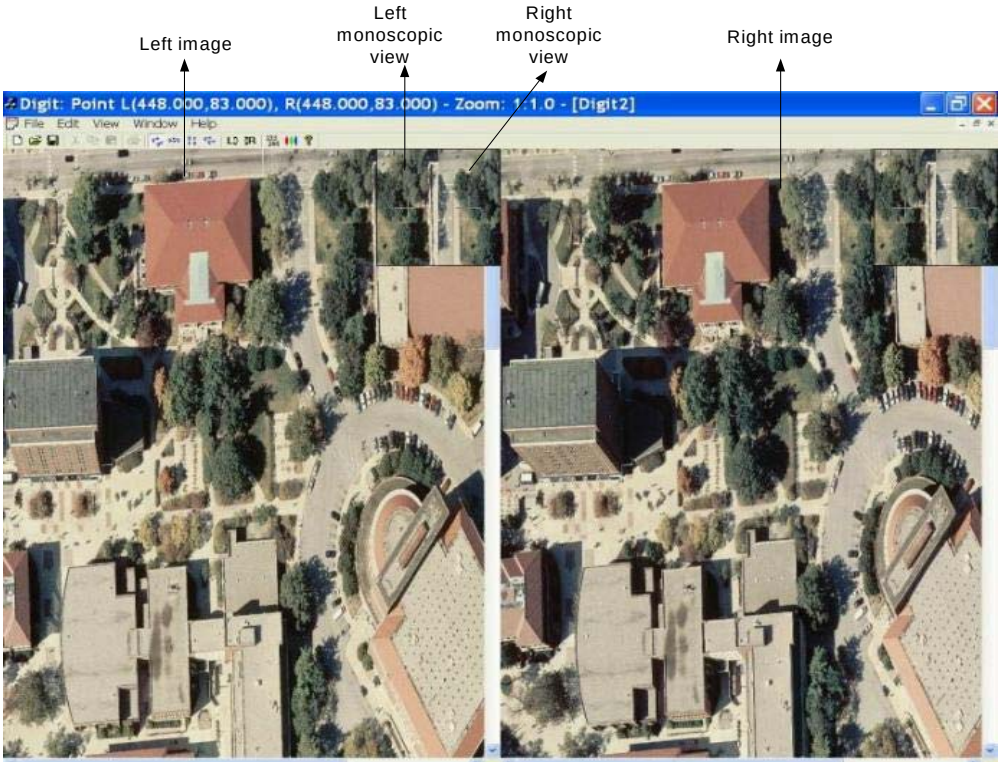


**Figure 9**. Auto3D measurement interface (Purdue campus images, 2D mode)

Another fundamental distinction in 3D autostereoscopic measurement is the dual and unsymmetrical design of graphic interface. Because any graphics will be viewed in 3D mode during the process of autostereoscopic measurement, they need to be designed identically and duplicated for each image window. Moreover, the column-interleave property also requires an unsymmetrical shape in 2D to achieve a symmetric appearance in 3D. Shown in Figure 10 are the designed point symbols in the left and right windows for 3D measurement. Two identical shapes should be used respectively for the left and right windows. Notice the symbol is not symmetric in geometry – an ellipse with major axis in vertical direction is used. However, they will appear as a circular symbol when being viewed in the autostereoscopic mode. This requirement would eventually double the work for the development of an autostereoscopic measurement tool.

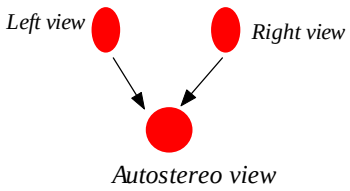


**Figure 10.** Dual and unsymmetrical graphic design

As a preprocessing process, Auto3D provides two options to prepare the image files required by 3D display. In the first option, one may duplicate the input image rows to double the vertical resolution. As an alternative, one may retain the odd columns of the left image and even columns of the right image to make the horizontal resolution half of the input images. To facilitate quality 3D view, the toolkit provides a set of image manipulation capabilities. These functions include rotation and vertical image movement. They are useful for removing y-parallax and making the photo base parallel to the eye base. Besides, users can display, locate, and edit the point symbols. Properties of labels can be changed, colored, stored into a file, and later loaded to continue by adding new measurements or editing existing measurements. These functions ultimately can be used to collect image features and determine their 3D ground truth. The following graphics and list in Figure 11 are a summary of Auto3D main functions.

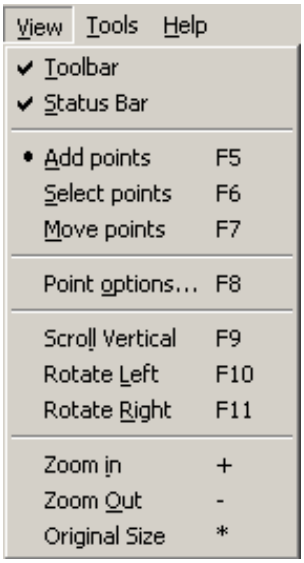


The application's menus and toolbar list the following function:

1. Image view operations:
    1) Zoom In
    2) Zoom out
    3) Original Size
2. Points editing:
    1) Add points
    2) Select points
    3) Move points
    4) Point options.
3. Image processing:
    1) Scroll Vertical
    2) Rotate Left
    3) Rotate Right

**Figure 11.** List of Auto3D toolkit functions

**Figure 12.** Examples of selected feature points for measurement (top: ground; bottom: roof)

## TESTS AND EVALUATION

In order to evaluate the performance of autostereoscopic measurement, a stereo pair over Purdue University campus is used to conduct autostereoscopic measurement tests. The original photo scale is about 1:4000 and scanned at a resolution of 33 μm. They are first epipolar normalized to remove possible y-parallax. The normalized images are then resampled to two resolutions, one at pixel size 25 μm, one at pixel size 50 μm, which will be used as the test images in our study.

Two types of well-defined feature points are selected for measurement. They consist of 18 points on the ground and 18 points on building roofs. Seven geomatics engineering major graduate students without intensive stereoscopic training are involved in the tests. They are asked to measure all 36 feature points at two resolutions (25μm and 50μm) by following the specification prepared by the test organizer. In the specification, the exact location of each feature point is verbally described and illustrated with an image clip of 150x150 pixels. Figure 12 presents some of the selected feature points to be measured in the tests.

Table 2 presents the statistics of the autostereoscopic measurements. The values in the table are calculated in the following way. The range reflects the maximum difference among the 7 observers, namely, the difference between the maximum measured coordinate and minimum measured coordinate. The mean of such ranges at 18 roof and 18 ground points are the listed mean-range values in Table 2. The standard deviation is the variation of 7 viewers at the 18 ground and 18 roof points, respectively. Such statistics are made respectively for the *x* coordinate measurements in the left and right image respectively. Since the images are normalized, their *y* values are then set as the same.

**Table 2.** Statistics of autostereoscopic measurements (in pixels, 25μm /50μm)

| | | x-left | x-right | y-both | Average |
|---|---|---|---|---|---|
| **Ground (18 points)** | **Mean-range** | 3.495/2.429 | 3.898/2.097 | 4.217/2.459 | 3.870/2.328 |
| | **Std. dev.** | 1.353/0.954 | 1.467/0.832 | 1.586/0.941 | 1.472/0.910 |
| **Roof (18 points)** | **Mean-range** | 4.343/2.144 | 3.014/2.432 | 4.4/2.878 | 3.919/2.485 |
| | **Std dev.** | 1.546/0.860 | 1.156/0.879 | 1.655/1.141 | 1.468/0.968 |

A few conclusions can be drawn from Table 2. First, the statistics from roof and ground measurements are very close. This suggests no significant difference in the precision of the two types of observations. In other words, the autostereoscope can accommodate large perception depths. Second, the measurement precision decreases as the image resolution reduces. However, this is not at the same rate. Our results indicate that the precision decreases only by a factor of 1.6 while the resolution reduces from 25μm to 50μm by a factor of 2. This is a good property when handling a large volume of data with limited resources and with the expectation of no significant loss in photogrammetric accuracy. Moreover, this property can also benefit fast and smooth image roaming during the measurement process. The third observation drawn from Table 2 is related to the consistency of measurement of different observers. The measurement difference among the seven observers is maximum 3.9 and 2.3 pixels, with a standard deviation of 1.5 and 0.9 pixels, respectively for the 25μm and 50μm resolution images. The range reflects the possible maximum errors in point identification and precision 3D perception among all the seven participant observers. The standard deviation suggests that the statistical consistency among the participants is at the range of 0.9-1.5 pixels, which agree with the property of the on-screen measurement process that has a one-pixel expected measurement uncertainty. The distribution of the measurement inconsistency is our fourth observation. It is very worthwhile noticing that the maximum difference (range) of measurement errors is about 2.6 constant times the corresponding standard deviation. This fact is found to be true for all the scenarios in our tests: two types of features at two different resolutions. It essentially suggests that our measurement errors are consistent and follow the same or very similar distribution. Finally, it should be noted that some points are difficult to digitize because of the low color contrast or ambiguous definition and interpretation on their precise locations.

## CONCLUSIONS

Barrier based autostereoscopic technology is currently an affordable and suitable option for goggle-free 3D image interpretation and photogrammetric measurement. The viewing effect is dependant on the design and specification of the 3D display. Viewers can obtain clear and correct stereo effect in a series of viewing zones of diamond shape. Analytical study shows this viewing zone can be as large as 13 cm in depth and minimum 7 locations in lateral. This restricts the viewer's freedom of movement while conducting autostereoscopic image interpretation and measurement. Autostereoscopic measurement follows a principle similar to the common goggle based measurement, however, with many distinctions. The two floating cursors must be fixed at a constant distance while images are being relatively moved to achieve 3D measurement. The images to be viewed in 3D mode should have a horizontal resolution half of the vertical one to accommodate the column interleave requirement. All graphics, including cursors, symbols, user interface graphics need to be designed in a dual and unsymmetrical manner, which eventually may complicate the application development. Our tests with the Auto3D toolkit suggest the autostereoscopic technology can accommodate large perception depth and yield similar measurement precision for

features at different elevations. Changes in image resolution cause measurement precision change in an unequally proportional manner. This is a good property when handling a large volume of data with limited resources and with the expectation of no significant loss in photogrammetric accuracy. Finally, the standard deviations of 0.9-1.5 pixels suggest the statistical consistency in the measurements of all the test participants. Further studies are needed to compare the same measurements with results from ordinary stereoscopic equipment and enhance current Auto3D capabilities with stereo feature extraction functions.

## REFERENCES


[1] Eichenlaub, Jesse b. (1991). Progress in autostereoscopic display technology at Dimension Technologies Inc., *SPIE Proceedings, Stereoscopic Displays and Applications II,* Editors, John O. Merritt, Scott S. Fisher, Vol. 1457, pp. 290-301, February, 25-27, 1991, San Jose, California.

[2] Eichenlaub, Jesse b. (1992). Further advances in autostereoscopic technology at Dimension Technologies Inc., SPIE Proceedings, Stereoscopic Displays and Applications III, Editors, John O. Merritt, Scott S. Fisher, Vol. 1669, 163-175. February, 12-13, 1992, San Jose, California.

[3] Merritt, John O., Scott S. Fisher, chairs/editors (1993). Stereoscopic displays and applications IV: 1-2 February, San Jose, California, sponsored by SPIE--the International Society for Optical Engineering, IS&T--the Society for Imaging Science and Technology.

[4] Lipton, L., (1992). Future of autostereoscopic electronic display, SPIE Proceedings, Stereoscopic Displays and Applications III, Editors, John O. Merritt, Scott S. Fisher, Vol. 1669, pp. 156-162. February, 12-13, San Jose, California.

[5] Fowles, G. R., (1989) Introduction to Modern Optics. Dover Publications, Inc., New York, 2nd edition.

[6] Hattori, Tomohiko (1991). Electro optical autostereoscopic displays using large cylindrical lenses, SPIE Proceedings, Stereoscopic Displays and Applications II, Editors, John O. Merritt, Scott S. Fisher, Vol. 1457, 283-289, February, 25-27, San Jose, California.

[7] Okoshi, T. (1976). Three Dimensional Imaging Techniques, Academic Press New York.

[8] Okoshi, T. (1980). Three Dimensional Displays. Proc. IEEE Vol. 68, 548-64.

[9] Petrie, G. (2001). 3D Stereo-Viewing of Digital Imagery: Is Auto-Stereoscopy the Future for 3D?, GeoInformatics, Vol. 4, No. 10, 24-29.

[10] Son, J., Saveljev, V. V., Choi, Y., Bahn, J., Kim, S., Choi, H. (2003) Parameters for designing autostereoscopic imaging systems based on lenticular, parallax barrier, and integral photography plates, Opt. Eng. 42(11), 3326-3333.


## APPENDIX

This appendix derives the analytical expression of viewing geometry. Figure 6 shows the geometry of viewing zone for a planar autostereoscopic display. For simplicity we consider the geometry in a horizontal plane passing the display center. The coordinate system is originated at the center of display, the axis x is parallel to the display plane, and the axis z is perpendicular to the display plane. The viewer's eyes, left ( L ) and right ( R ), are separated by the distance, e, and at a viewing distance, v, from the display plane. In Figure 6, S1 is the screen right end, while S2 is screen left end. w is the screen width. The front triangle right next to the center line is ΔABC defined by the intersection of lines from S1, S2 and z = v.

Equation of line $\overline{S_1 B}$ , passing through point (0, v) and ( $\frac{w}{2}$ , 0)

$$z = \frac{-2v}{w} x + \frac{wv}{w} \tag{A-1}$$

Equation of line $\overline{S_2 C}$ , passing through point (e, v) and (- $\frac{w}{2}$ , 0)

$$z = \frac{2v}{w+2e} x + \frac{wv}{w+2e} \tag{A-2}$$

Solving Equation (A-1) and (A-2) will yield the location of point A as ( $\frac{we}{2(w+e)}$ , $\frac{wv}{w+e}$ ). Similarly, this

equation can be generalized to the triangle *n*, whose front node's coordinates will be $(\frac{(2n-1)we}{2(w+e)}, \frac{wv}{w+e})$.

For the rear triangle, Equation of line from $\overline{S_2B}$, passing through point (0, v), $(-\frac{w}{2}, 0)$

$$z = \frac{2v}{w+e}x + \frac{wv}{w+e} \tag{A-3}$$

Equation of line $\overline{S_1C}$, passing through point (e, v), $(\frac{w}{2}, 0)$

$$z = \frac{-2v}{w-2e}x + \frac{wv}{w-2e} \tag{A-4}$$

From equation (A-3), (A-4) we can get the coordinate of point D as $(\frac{we}{2(w-e)}, \frac{wv}{w-e})$ and, we can also extend the geometry relationship to triangle *n* as $(\frac{(2n-1)we}{2(w-e)}, \frac{wv}{w-e})$.

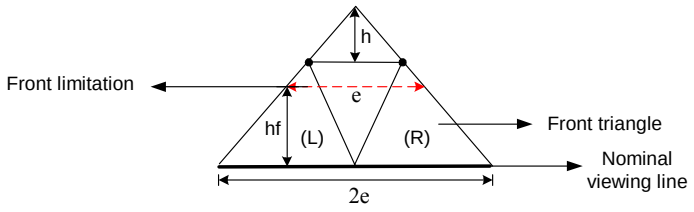


**Figure A.** Geometry of front triangle and the limitation of viewer's movement

Front limitation ($h_f$) as shown in figure A, from the similar triangle geometry:

$$\frac{h}{\frac{we}{w+e}} = \frac{h + (v - \frac{wv}{w+e})}{2e}$$

This will lead to the front head movement range/height

$$h_f = \frac{ev}{w+2e} \tag{A-5}$$

Similarly, we can obtain the relationship for the rear triangle

$$\frac{h_r}{e} = \frac{\frac{wv}{w-e} - v}{\frac{we}{w-e}}$$

This will yield to the rear head movement range/height

$$h_r = \frac{ev}{w} \tag{A-6}$$